Frequency-Dependent Coupling and Interaction Suppression of GFM and GFL Inverters

Zimin Jiang and Peng Zhang

***Abstract*—With the increasing penetration of inverter based resources (IBRs), inverter control methods, including grid-following (GFL) and grid-forming (GFM) control, dominate the dynamic characteristics of power systems. The difference in control methods creates a more complex interaction coupling between them and significantly affects the dynamic stability and performance of the system. This paper aims to reveal the interaction mechanisms of the GFM and GFL inverters and develop control strategies to suppress these interactions. A dynamic relative gain array-based method is developed to quantify frequency-dependent coupling between any specified control loops of GFL and GFM inverters under varying grid conditions and control parameters. Based on the identified interaction, a port-Hamiltonian-based control method, which encodes the inverter controller structure, is devised to suppress the interactions under varying operating conditions without incurring new instability issues. Experimental results verify both the interaction analysis and the effectiveness of the designed suppression strategy.**

***Index Terms*—Inverter interaction, grid following, grid forming, dynamic relative gain array, port-controlled Hamiltonian**

I. INTRODUCTION

Grid-forming (GFM) inverters are deployed to enhance the stability of power systems with grid-following (GFL) inverters [1], [2], leading to the evolution of a heterogeneous system comprising both GFM and GFL units. In such systems, there exists interaction within and between inverters, which collectively determine their dynamic characteristics and stability [3], [4]. Differences in GFM and GFL control create a more complex interaction coupling between them under evolving grid conditions, negatively impacting GFM inverters' support capabilities and aggravating instability [5], [6]. Therefore, it is essential to elucidate the interaction mechanisms of GFM and GFL inverters [7] and to develop suppression strategies to suppress these interactions.

Existing studies on the stability of heterogeneous inverter systems can generally be divided into two categories: state-space model-based methods [8], [9] and impedance model-based methods [6], [10]. In literature [9], a state-space model-based approach is used to quantitatively investigate the impact of parameters on hybrid system interactions using participation factors; however, interactions among control loops are not considered. The impedance model-based method in [10] examines how the number of GFM and GFL inverters affects interaction but lacks quantitative analysis. Varying grid strength, inappropriate control parameters and line parameters can also impact interactions. A comprehensive and quantitative analysis of interactions among inverters under different grid strengths is yet to be conducted. Existing suppression approaches include damping modification, virtual impedance adjustment, energy-based method, or their combinations [8]. However, these methods may fail under varying grid conditions. Thus, it is still necessary to devise suppression methods that can maintain stability across a range of operating conditions.

To bridge the gaps, this paper reveals the interaction mechanism of GFM and GFL inverters and devises an effective interaction suppression method for hybrid systems under varying grid conditions. Our contributions include: 1) A dynamic relative gain array (DRGA)-based method is devised to quantitatively evaluate the interaction between any specified control loops of GFM and GFL inverters under varying control parameters and grid conditions; 2) A port-Hamiltonian-based control encoding inverter controller structure is devised to suppress these interactions. Theoretical analysis and the devised suppression method are verified by experimental tests.

The remainder of this paper is organized as follows: Section II presents the devised DRGA-based interaction analysis method. Section III provides the port-Hamiltonian-based interaction suppression method. The experimental results validating the theoretical analysis and the effectiveness of the interaction suppression method are reported in Section IV. Section V concludes the paper.

II. DYNAMIC RELATIVE GAIN ARRAY-BASED FREQUENCY-DEPENDENT COUPLING ANALYSIS

Grid-connected inverters are mainly of two types, i.e., GFL and GFM inverters. GFL inverters usually employ the PQ-control to inject power to the grid by following the measured voltage at its terminal [11]. GFM inverters regulate frequency and voltage via droop control [12] or virtual synchronous machine control [1] to enhance system stability under weak grid conditions. Without loss of generality, a hybrid power system comprising droop-controlled GFM inverters and PQ-controlled GFL inverters can be modeled as a multiple-input-multiple-output (MIMO) system using state-space equations as follows

$$\begin{cases} \dfrac{d\boldsymbol{x}}{dt} = \boldsymbol{A}\boldsymbol{x} + \boldsymbol{B}\boldsymbol{u} \\ \boldsymbol{y} = \boldsymbol{C}\boldsymbol{x} + \boldsymbol{D}\boldsymbol{u} \end{cases} \tag{1}$$

This work relates to the Department of Navy award N000142512374 issued by the Office of Naval Research. The United States Government has a royalty-free license throughout the world in all copyrightable material contained herein. *Corresponding Author: Peng Zhang.*

The authors are with the Department of Electrical and Computer Engineering, Stony Brook University, NY 11794-2350 USA (e-mails: zimin.jiang, p.zhang@stonybrook.edu).

979-8-3315-8138-1

where $\boldsymbol{x} \in \mathbb{R}^m$, $\boldsymbol{u} \in \mathbb{R}^n$ and $\boldsymbol{y} \in \mathbb{R}^l$ are the state variables, input variables and output variables, respectively. $\boldsymbol{A} \in \mathbb{R}^{m\times m}$, $\boldsymbol{B} \in \mathbb{R}^{m\times n}$, $\boldsymbol{C} \in \mathbb{R}^{l\times m}$ and $\boldsymbol{D} \in \mathbb{R}^{l\times n}$ are the system, input and output matrices respectively. m, n and l denote the number of the state, input and output variables. The dynamic characteristics of a multi-inverter system can be analyzed with matrices $\boldsymbol{A}$ and $\boldsymbol{B}$.

The transfer function of a hybrid system described by Eq. (1) is calculated as

$$\boldsymbol{H}_{sys} = \frac{\boldsymbol{y}(s)}{\boldsymbol{u}(s)} = \boldsymbol{C}(s\boldsymbol{I} - \boldsymbol{A})^{-1}\boldsymbol{B} + \boldsymbol{D} \tag{2}$$

The $\boldsymbol{H}_{sys}$ is a frequency-domain matrix, thus, it can be used to quantitatively evaluate the coupling interaction between control loops of different frequency ranges.

DRGA quantifies the interactions between specified control loops of GFM and GFL inverters by analyzing the relationships between the corresponding inputs $\boldsymbol{u}$ and outputs $\boldsymbol{y}$ at selected frequency ω [13] with the following equation

$$\lambda_{ij} = \frac{N_{ij}}{M_{ij}} = \frac{[\Delta y_i(j\omega)/\Delta u_j(j\omega)]_{\Delta u_k=0,\, k\neq j}}{[\Delta y_i(j\omega)/\Delta u_j(j\omega)]_{\Delta y_k=0,\, k\neq i}} \tag{3}$$

where $\lambda_{ij}(j\omega)$ denotes the dynamic relative gain of the selected control loop at ω, its value indicates the extent to which one control loop is influenced by another. N_{ij} and M_{ij} represent the gains when other loops are open and closed, respectively. For an MIMO system with a transfer function $\boldsymbol{H}(s)$, the DRGA of the system can be obtained by

$$\boldsymbol{\Lambda}(s) = [\lambda_{ij}(s)] = \boldsymbol{H}(s) \odot \boldsymbol{H}^{-T}(s) \tag{4}$$

where $\odot$ is the Hadamard product and $\boldsymbol{\Lambda}(s)$ is the DRGA of the system composed of $\lambda_{ij}(s)$.

Given the power grid's model in Eqs. (1) and (2), the interaction between any specified loops of GFM and GFL inverters can be quantitatively assessed. Moreover, the influence of varying parameters, e.g., grid strength and control parameters, on the interaction of specified control loops in the frequency range $[f_{min}, f_{max}]$ can also be effectively evaluated. The rule for interaction analysis using the DRGA-based method is [13]:

- When $\lambda_{ij} > 1$, strong coupling exists between the corresponding loops, meaning that dynamics or disturbances in other loops significantly influence the selected loop. The larger the value of $\lambda_{ij} > 1$, the stronger the interaction between them.
- When $0 < \lambda_{ij} < 1$, the interaction between the corresponding loops is weak across the relevant frequency range.

III. Port-Hamiltonian based Interaction Suppression Method

The DRGA-based method in Section II can be used to identify the interaction between any specified control loops. A suppression method taking into consideration of the inverter control structure can effectively mitigate the interactions without tuning the system with trial and error and incurring new instability issues under varying grid conditions. A port-controlled Hamiltonian based method is devised to suppress these interactions in this section.

A port-controlled Hamiltonian reflecting the dynamics of a hybrid system is given as

$$\dot{x} = [\mathcal{J}(x) - \mathcal{R}(x)]\frac{\partial H(x)}{\partial x} + g(x)u, y = g^T(x)\frac{\partial H(x)}{\partial x} \tag{5}$$

where $H(x)$ is a function defining the system energy, $\mathcal{J}(x)$ and $\mathcal{R}(x)$ are the interconnection and damping matrices, respectively, $\mathcal{R}(x) = \mathcal{R}^{\mathrm{T}}(x) \geq 0$ and $\mathcal{J}(x) = -\mathcal{J}^{\mathrm{T}}(x)$, $g(x)$ is the input matrix. The port-controlled Hamiltonian framework supports modular formulation, meaning it enables the synthesis of a global control strategy for all systems based on a single inverter indexed by i, i.e., $\dot{x}_i = [\mathcal{J}_i(x_i) - \mathcal{R}_i(x_i)]\nabla H_i(x_i) + g_i(x_i)u_i$.

To suppress the identified interactions, the idea is to design a feedback control law of the form $u(x) = \beta(x)$ for the port-controlled Hamiltonian system in Eq. (5), ensuring that the closed-loop dynamics still preserve the port-controlled Hamiltonian form while achieving the desired dynamic performance, which is given as

$$\dot{x}_i = [\mathcal{J}_{di}(x) - \mathcal{R}_{di}(x)]\frac{\partial H_{di}(x)}{\partial x} \tag{6}$$

where $\mathcal{J}_{di}(x) = -\mathcal{J}_{di}^{\mathrm{T}}(x)$ and $\mathcal{R}_{di}(x) = \mathcal{R}_{di}^{\mathrm{T}}(x) \geq 0$ denote the desired interconnection and damping matrices, respectively; and $H_{di}(x)$ is the desired energy function having a strict local minimum at the equilibrium point x^*.

Consider $\mathcal{J}_i(x_i), \mathcal{R}_i(x_i), H(x), g(x)$ and the desired equilibrium x^* to be stabilized. Assume that there exists $\mathcal{J}_{di}(x), \mathcal{R}_{di}(x)$ and $H_{di}(x)$, then Eq. (7) holds [14]

$$\begin{aligned}[\mathcal{J}_i(x_i) - \mathcal{R}_i(x_i)]\frac{\partial H_i(x)}{\partial x} + g_i(x_i)u_i \\ = [\mathcal{J}_{di}(x) - \mathcal{R}_{di}(x)]\frac{\partial H_{di}(x)}{\partial x}\end{aligned} \tag{7}$$

Given Eq. (7), the control law can then be obtained as [14]

$$\begin{aligned}u = \underbrace{\left[g^\top(x)g(x)\right]^{-1}g^\top(x)}_{\text{gain term}}\Big[\big(J_d(x) - R_d(x)\big)\frac{\partial H_d(x)}{\partial x} \\ - \big(J(x) - R(x)\big)\frac{\partial H(x)}{\partial x}\Big]_{\beta(x)}\end{aligned} \tag{8}$$

With u, the closed-loop system is passive and stable. Note that if $x*$ is the largest invariant subset in $\{x \in \mathcal{X} | \frac{\partial H_d^\top}{\partial x}(x)\mathcal{R}_d(x)\frac{\partial H_d}{\partial x}(x) == 0\}$, x^* is asymptotically stable. This conclusion holds globally if x^* is a global minimum of a radially unbounded $H_d(x)$ [14].

The desired functions can be chosen as the sum of the functions $\mathcal{J}_i(x_i)$, $\mathcal{R}_i(x_i)$, $H(x)$, and auxiliary functions $\mathcal{J}_{ai}(x_i)$, $\mathcal{R}_{ai}(x_i)$, $H_{ai}(x)$ such that

$$\begin{aligned}\Big[(\mathcal{J}_i(x_i) + \mathcal{J}_{ai}(x_i)) - (\mathcal{R}_i(x_i) + \mathcal{R}_{ai}(x_i))\frac{\partial H_{ai}(x)}{\partial x_i}\Big] \\ = -[\mathcal{J}_{ai}(x_i) - \mathcal{R}_{ai}(x_i)]\frac{\partial H_i(x)}{\partial x_i} + g_i(x_i)u_i(x_i)\end{aligned} \tag{9}$$

979-8-3315-8138-1

To ensure that the closed-loop system maintains the port-controlled Hamiltonian form and achieves the desired dynamics, these auxiliary terms used to assign the desired functions should be properly selected, fulfilling the conditions implicitly stated in [14].

For a GFM inverter connected to the grid through an LCL filter and equipped with droop and virtual impedance control, the candidate Hamiltonian function can be defined as

$$H_i(x_i) = \frac{1}{2}(L_{fi}i_{di}^2 + L_{fi}i_{qi}^2 + C_{fi}v_{Cdi}^2 + C_{fi}v_{Cqi}^2 + \xi_{pi}\omega_i^2 + \xi_{qi}E_i^2 + L_{vi}i_{Ldi}^2 + L_{vi}i_{Lqi}^2) \quad (10)$$

with the vector of the state variable being $x_i = M_i[i_{di}\ i_{qi}\ v_{Cdi}\ v_{Cqi}\ \omega_i\ E_i\ i_{Ldi}\ i_{Lqi}]^{\mathrm{T}}$, $M_i = \mathrm{diag}\{L_{fi}\ L_{fi}\ C_{fi}\ C_{fi}\ \xi_{pi}\ \xi_{qi}\ L_{vi}\ L_{vi}\}$ and $H_i(x) = (1/2)x_i^{\mathrm{T}}M_i^{-1}x_i$. ξ_{pi} and ξ_{qi} denote the time constant of the low-pass filter associated with the droop control loop. $\mathcal{J}_i(x_i)$ is expressed as

$$\mathcal{J}_i(x_i) = \begin{bmatrix} 0 & L_{f_i}\omega_i & -1 & 0 & 0 & 0 & 0 & 0 \\ -L_{f_i}\omega_i & 0 & 0 & -1 & 0 & 0 & 0 & 0 \\ 1 & 0 & 0 & C_{f_i}\omega_i & 0 & -1 & 0 & 0 \\ 0 & 1 & 0 & -C_{f_i}\omega_i & 0 & 0 & -1 & 0 \\ 0 & 0 & 0 & 0 & 0 & 0 & 0 & 0 \\ 0 & 0 & 0 & 0 & 0 & 0 & 0 & 0 \\ 0 & 0 & 1 & 0 & 0 & 0 & 0 & 0 \\ 0 & 0 & 0 & 1 & 0 & 0 & 0 & 0 \end{bmatrix} \quad (11)$$

$\mathcal{R}_i(x_i) = \mathrm{diag}\{R_{fi}\ \ R_{fi}\ \ 0\ \ 0\ \ 1\ \ 1\ \ Z_{vi}\ \ Z_{vi}\}$. R_{fi} and Z_{vi} are the filter resistance and virtual impedance respectively.

$H_{di}(x)$ should have a strict local minimum at the equilibrium point x^*, which can be chosen as

$$H_{di}(x_i) = \frac{1}{2}[L_{fi}(i_{di} - i_{di}^*)^2 + L_{fi}(i_{qi} - i_{qi}^*)^2 + C_{fi}(v_{Cdi} - v_{Cdi}^*)^2 + C_{fi}(v_{Cqi} - v_{Cqi}^*)^2 + \xi_{pi}(\omega_i - \omega_i^*)^2 + \xi_{qi}(E_i - E_i^*)^2 + L_{vi}(i_{Ldi} - i_{Ldi}^*)^2 + L_{vi}(i_{Lqi} - i_{Lqi}^*)^2] \quad (12)$$

Considering the initial form of $\mathcal{J}_i(x_i)$ and $\mathcal{R}_i(x_i)$, the new desired matrices $\mathcal{J}_{di}(x_i)$ and $\mathcal{R}_{di}(x_i)$ can be selected as

$$\mathcal{J}_{di}(x_i) = \begin{bmatrix} 0 & 0 & p_{13i} & 0 & 0 & 0 & 0 & 0 \\ 0 & 0 & 0 & p_{24i} & 0 & 0 & 0 & 0 \\ p_{31i} & 0 & 0 & 0 & 0 & 0 & p_{37i} & 0 \\ 0 & p_{42i} & 0 & 0 & 0 & 0 & 0 & p_{48i} \\ 0 & 0 & 0 & 0 & 0 & 0 & 0 & 0 \\ 0 & 0 & 0 & 0 & 0 & 0 & 0 & 0 \\ 0 & 0 & p_{73i} & 0 & 0 & 0 & 0 & 0 \\ 0 & 0 & 0 & p_{84i} & 0 & 0 & 0 & 0 \end{bmatrix} \quad (13)$$

and $\mathcal{R}_{di}(x_i) = \mathrm{diag}\{r_{11i}\ r_{22i}\ r_{33i}\ r_{44i}\ r_{55i}\ r_{66i}\ r_{77i}\ r_{88i}\}$, where $p_{ij} = -p_{ji}$ and $p_{ii} \geq 0$, $i,j \in \{1,\ldots,8\}$ for $i \neq j$. It can be noted obviously that $\mathcal{J}_{di}(x) = -\mathcal{J}_{di}^{\mathrm{T}}(x)$ and $\mathcal{R}_{di}(x) = \mathcal{R}_{di}^{\mathrm{T}}(x) \geq 0$ and preserves the structure. With the selected desired matrices, passivity of the desired port-controlled Hamiltonian is assured since

$$-\nabla_{x_i}^2 H_d(x_i^*) = -\frac{2}{L_{fi}} - \frac{2}{C_{fi}} - \frac{1}{\xi_{pi}} - \frac{1}{\xi_{qi}} - \frac{2}{L_{vi}} < 0 \quad (14)$$

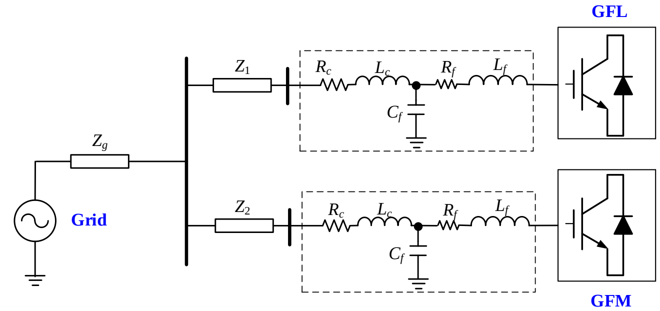

Fig. 1. Diagram of the test system.

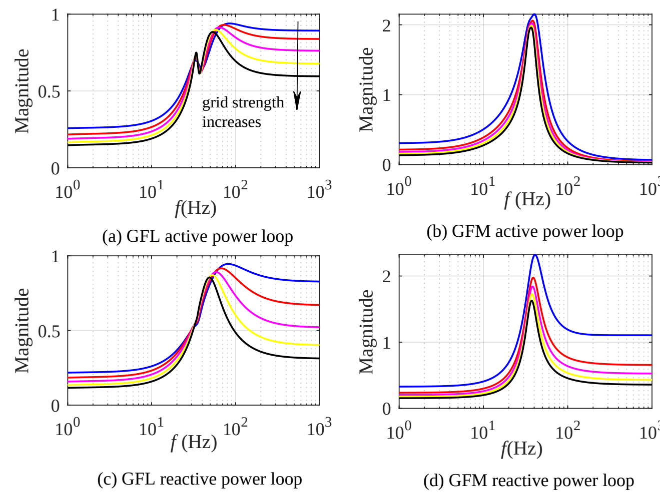

Fig. 2. Quantified interaction between power loops of GFM and GFL inverters under varying grid strength conditions.

The parameters in $\mathcal{J}_{di}(x)$ and $\mathcal{R}_{di}(x)$ correspond to the controller parameters of droop control, virtual impedance loop, voltage and current control loop, which can be tuned while ensuring passivity to suppress interactions between the control loops of GFM and GFL inverters identified by DRGA.

IV. Experimental Studies

A hybrid system with one GFM and one GFL inverter in parallel is studied with the grid modeled as an ideal voltage source in series with an impedance, as shown in Fig. 1. The controller parameters and grid impedance in p.u. values can be found in [1] and [15]. Considering the characteristics of GFM and GFL inverters, this section examines two critical scenarios, i.e., power coupling and $[P\,Q] - [\omega\,V]$ interaction.

A. Quantitative Interaction Analysis

1) Power Loop Interaction: The power loop interaction between the GFM and GFL inverters is examined first. The results of quantified interaction under different grid strengths are presented in Fig. 2. It can be observed from subfigures (a) and (c) that under a strong grid, the relative gain is smaller than 1 for frequencies between 1 to 1000 Hz, meaning the active and reactive power loops of the GFL inverter both exhibit negligible coupling. This is because a strong grid stabilizes the

979-8-3315-8138-1

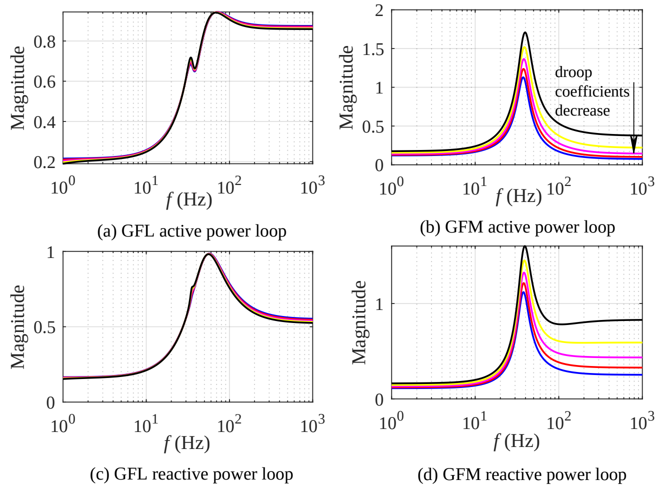

Fig. 3. Quantified interaction between power loops of inverters under different droop coefficients of the GFM inverter.

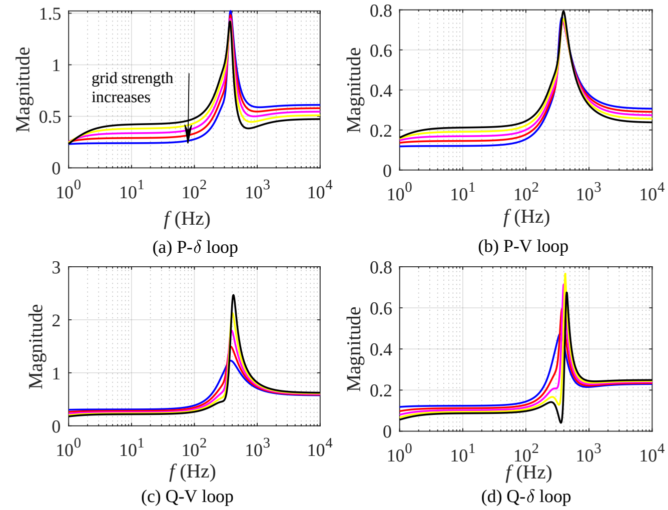

Fig. 4. Quantified interaction between the $[P\,Q]-[\omega\,V]$ loop of the GFM and GFL inverters.

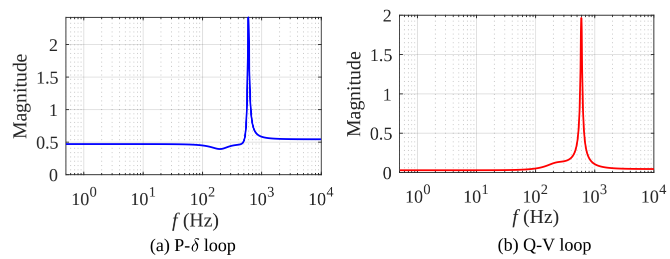

Fig. 5. Results of controller parameter tuning for suppressing interactions between GFM and GFL inverters.

point of common coupling (PCC) voltage against disturbances from the GFM inverter. As the grid strength decreases, as shown in subfigures (b) and (d), the relative gain is larger than 1 over portions of the frequency range, with a coupling peak at 35.1 Hz, which means the interaction between the GFL and GFM inverters will occur. The output of one inverter will be significantly affected when a disturbance or dynamic occurs on another inverter due to the reduced PCC voltage stiffness.

2) Effects of Droop Coefficients on Interactions: The devised DRGA-based method is used to study how the droop coefficients of the GFM inverter affect the interaction. Fig. 3 demonstrates the impact of droop coefficients on power loop coupling. The results of quantified interaction with different droop coefficients are shown in Fig. 3. As can be seen from subfigures (a) and (c), the coupling between the GFL and GFM inverters is almost unaffected by the droop coefficients over the considered frequency range, as the relative gain remains below 1. Changing droop coefficients mainly affects the coupling characteristics of the GFM inverter's power loops, as demonstrated in subfigures (b) and (d). Reducing the droop coefficients can alleviate the interaction, but the relative gain exceeds 1 over a specific range of frequencies. Changing the droop coefficients can significantly affect the overall performance of the system, e.g., power sharing; therefore, it still requires a suppression method to stabilize the system.

3) $[P\,Q]-[\omega\,V]$ Interaction: The interaction between the $[P\,Q]-[\omega\,V]$ loop directly reflects the grid support capability of the GFM inverter to stabilize the system. The results of quantified interaction analysis under different grid strengths are shown in Fig. 4. As the grid strength decreases, the coupling between the $P-\omega$ and $Q-V$ intensifies because the relative gain increases, as can be seen in subfigures (a) and (c). Strong couplings exist over portions of the considered frequency range as the relative gain value exceeds 1, with a coupling peak at 318.2 Hz. But it can be observed from subfigures (b) and (d) that the coupling between the $P-V$ and $Q-\omega$ loop is negligible under the considered grid strengths, since the relative gain remains below 1 under all considered frequencies. This complies with the droop control strategy applied by the GFM inverter.

B. Port-Hamiltonian based Interaction Suppression

1) Incompetence of Tuning Parameters for Suppressing Interaction: First, we show that new interactions can be introduced with only tuning controller parameters. As the interaction between the $[P\,Q]-[\omega\,V]$ loop in Fig. 4, the inner loop and the virtual impedance loop are tuned to mitigate it. The calculated relative gain of the $P-\delta$ and $Q-V$ loops is shown in Fig. 5. In comparison to the results in Fig. 4, the relative gain at 318.2 Hz is below 1, which means the interaction is suppressed. However, new interactions at higher frequencies are introduced, as the relative gain exceeds 1 over a range of increased frequency. In a work, there is a risk of introducing new interactions with tuning parameters only, and a suppression method is still necessary to stabilize the system.

2) Suppression with the Devised Method: To validate the power loop interaction identified in Fig. 2, a disturbance is added to the active power reference of the GFM inverter. The experimental results without and with the devised suppression method are shown in Fig. 6. It can be seen that the disturbance at 35.1 Hz on the output power of GFM inverter is clearly observed, which confirms the interaction analysis. It means the system intensifies external disturbances

979-8-3315-8138-1

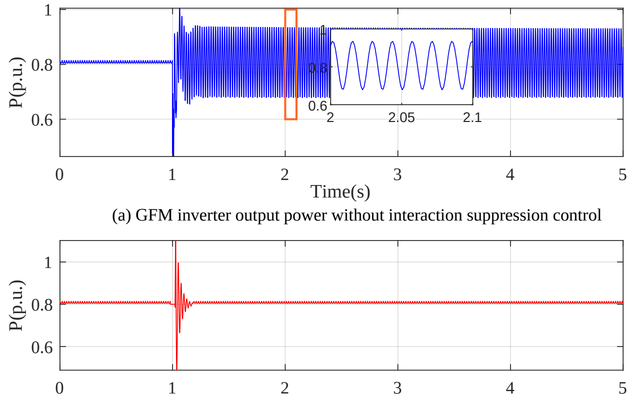

(a) GFM inverter output power without interaction suppression control

(b) GFM inverter output power with interaction suppression control

Fig. 6. Results of suppression control for the GFM inverter power loop.

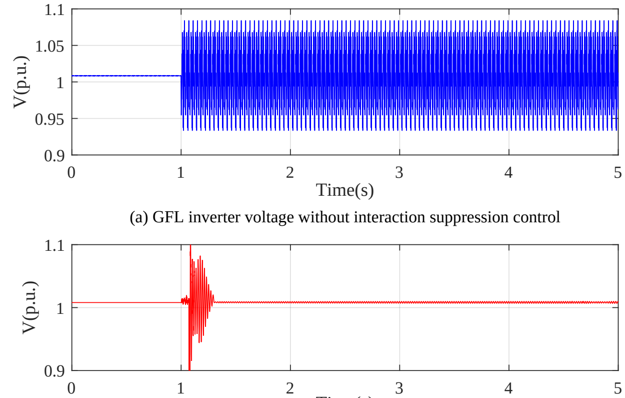

(a) GFL inverter voltage without interaction suppression control

(b) GFL inverter voltage with interaction suppression control

Fig. 7. Results of suppression control for the $[P\, Q] - [\omega\, V]$ interaction.

and lacks damping capability, resulting in instability to low-frequency disturbances. The testing result with the devised suppression method is shown in Fig. 6 (b). It can be seen that the interaction is damped when applying the same disturbance to the GFM inverter, which validates the effectiveness of the devised method.

For the $[P\, Q] - [\omega\, V]$ interaction, a disturbance on the GFM inverter reactive power control loop is created, the output voltage of the GFL inverter is shown in Fig. 7 (a). It can be observed that the interaction between the $Q - V$ loop is excited due to the resulted oscillation of the GFL inverter's output voltage. GFM inverter regulates the voltage and can thus significantly affect the GFL inverter. Therefore, there exists a strong coupling between $[P\, Q] - [\omega\, V]$ loop, validating the correctness of the theoretical analysis. To suppress the coupling between the GFM inverter and the GFL inverter, voltage feedback control and damping control can easily be implemented with the port-controlled Hamiltonian method to encode the controller structure. The results of the suppression control are shown in Fig. 7 (b). It can also be seen that the interaction is effectively suppressed and the system is stable after applying the same disturbance. The testing results verify the effectiveness of the devised method.

V. Conclusion

To clarify the interaction mechanism of GFM and GFL inverters and develop an effective interaction suppression method, this paper devises a DRGA-based method to quantitatively analyze interactions in hybrid systems. The frequency-dependent interactions between control loops are analyzed, along with the influence of key parameters under varying grid conditions. With the identified coupling control loops, the devised port-Hamiltonian-based control can encode the inverter controller structure directly to suppress these interactions. Theoretical analysis and the devised suppression method are validated by experimental tests. Future research will focus on interaction analysis and practical suppression design for large-scale IBR-dominated power systems under uncertainties.

References

[1] Z. Jiang, P. Zhang, Y. Zhou, L. Kocewiak, D. K. Chandrashekhara, M.-L. Picherit, Z. Tang, K. B. Bowes, and G. Yang, "Software-defined virtual synchronous condenser," *IEEE Transactions on Power Systems*, vol. 40, no. 2, pp. 1255–1268, 2025.

[2] N. Nikmehr, M. A. Bragin, P. Zhang, and P. B. Luh, "Computationally distributed and asynchronous operational optimization of droop-controlled networked microgrids," *IEEE Open Access Journal of Power and Energy*, vol. 9, pp. 265–277, 2022.

[3] L. Wang, Y. Zhou, W. Wan, H. Ye, and P. Zhang, "Eigenanalysis of delayed networked microgrids," *IEEE Transactions on Power Systems*, vol. 36, no. 5, pp. 4860–4863, 2021.

[4] P. Zhang, *Microgrids: Theory and Practice*. John Wiley & Sons, 2024.

[5] S. Dennetière, P. Rault, H. Saad, Y. Fillion, Sharifabadi, and *et al*, "Technical solutions to predict and mitigate inadvertent interaction of two parallel connected VSC-HVDC schemes feeding an islanded offshore oil and gas grid," in *Proceedings of the CIGRE Session*, 2020, pp. 1–16.

[6] Y. Wang, L. Ruan, M. Yang, X. Xiao, S. Chen, and O. Gomis-Bellmunt, "Control interaction analysis of hybrid system with grid-following and grid-forming inverters based on admittance decomposition," *Int. J. Electrical Power & Energy Systems*, vol. 162, p. 110267, 2024.

[7] P. Zhang, *Networked Microgrids*. Cambridge University Press, 2021.

[8] X. Liu, Y. Chen, Z. Wang, C. Luo, Z. Xie, Y. Fu, and X. Li, "Power oscillation analysis and dual mutual damping control for hybrid system with GFM and GFL inverters under varying short circuit ratio," *IEEE Trans. Power Syst.*, pp. 1–12, 2025.

[9] P. Sun and *et al*, "Dynamic interaction analysis and damping control strategy of hybrid system with GFM and GFL control modes," *IEEE Transactions on Energy Conversion*, vol. 38, no. 3, pp. 1639–1649, 2023.

[10] S. Jiang and G. Konstantinou, "Generalized impedance model and interaction analysis for multiple grid-forming and grid-following converters," *Electric Power Systems Research*, vol. 214, p. 108912, 2023.

[11] L. Kocewiak, R. Blasco-Giménez, C. Buchhagen, J. B. Kwon, Y. Sun, A. S. Trevisan, M. Larsson, and X. Wang, "Overview, status and outline of stability analysis in converter-based power systems," in *Proc. Virtual Wind Integr. Workshop*, 2020, p. 10.

[12] Y. Zhou and P. Zhang, "Neuro-reachability of networked microgrids," *IEEE Transactions on Power Systems*, vol. 37, no. 1, pp. 142–152, 2021.

[13] Y. A. Arkun, "Dynamic block relative gain and its connection with the performance and stability of decentralized control structures," *International Journal of Control*, vol. 46, no. 4, pp. 1187–1193, 1987.

[14] S. S.-E. Plaza, R. Reyes-Báez, and B. Jayawardhana, "Total energy shaping with neural interconnection and damping assignment-passivity based control," in *4th Annual Conference on Learning for Dynamics and Control*. PMLR, 2022, pp. 520–531.

[15] Y. Zhang, Y. Gu, Y. Zhu, T. C. Green, and H.-D. Chiang, "On the interaction in transient stability of two-inverter power systems containing GFL inverter using manifold method," *arXiv preprint arXiv:2501.05994*, 2025.

979-8-3315-8138-1